

Effect of Solvents on ZIF-8 and its Adsorption Efficiency for Norfloxacin

Li Li Wu^{1,2}, Huey Ling Tan^{1,*}, Ying Pei Lim¹

¹School of Chemical Engineering, College of Engineering, Universiti Teknologi MARA, Shah Alam, 40450 Selangor, Malaysia ²Department of Chemistry, Hengshui University, 053000, Hebei Province, Hengshui, China

*Corresponding Author's E-mail: hueyling@uitm.edu.my

Received: 03 February 2025 Accepted: 29 June 2025 Onlin First: 01 September 2025

ABSTRACT

In this study, ZIF-8, a novel adsorption material for norfloxacin (NOR) adsorption, was created and evaluated. This study aimed to investigate the effect of using different solvents – water and methanol during the synthesis process on the adsorption performance of ZIF-8 towards NOR. Fourier Transform Infrared (FTIR) spectroscopy, Scanning Electron Microscope (SEM) coupled with Energy Dispersive X-ray (EDX), Brunauer-Emmett-Teller (BET) and X-ray Diffractometer (XRD) studies were used to fully evaluate the synthesized adsorption material in order to comprehend its adsorption capabilities and structural characteristics. The findings indicated that ZIF-8 synthesized using methanol (ZIF-8-M) demonstrated superior crystallinity, greater pore volume, and a larger surface area when compared to ZIF-8-W, which was produced using water. Additionally, ZIF-8-W had a non-uniform particle structure with grain sizes of approximately 50.19±6.40 nm, while ZIF-8-M exhibited a uniform morphology with grain sizes around 12.62±1.11 nm. The adsorption experiments demonstrated that ZIF-8-M exhibited superior removal efficiency (86.4%) and adsorption capacity (17.30 mg g^{-1}) for NOR, while ZIF-8-W achieved lower values of 53.01% and 10.60 mg g⁻¹, respectively. In addition, isotherm studies demonstrated that both materials exhibited multilayer adsorption, with the Freundlich model best fit their adsorption behaviour. Using kinetic analysis, a pseudosecond-order model that suggested a chemical adsorption process was verified. Higher temperatures favoured adsorption, based on thermodynamic





study, which also identified the spontaneous and endothermic process. This research underscores the importance of solvent choice during the synthesis process, which can significantly affect the properties of ZIF-8. The findings provide an improved comprehension of how solvents and ZIF-8 interact, which could lead to more efficient solutions for mitigating pharmaceutical pollution in wastewater systems.

Keywords: Wastewater Treatment; Adsorption; NOR; ZIF-8; Solvent

INTRODUCTION

The increased use of antibiotics due to scientific advancements has raised concerns about human health risks and the emergence of antibiotic-resistance bacteria [1]. The indiscriminate use of antibiotics has led to a global health crisis characterized by chronic toxicity, disruption of aquatic ecosystems, and the emergence of antibiotic-resistant microorganisms [2]. The synthetic antibiotic norfloxacin (NOR), which is categorized as a third-generation quinolone, has a broad range of action [3]. By specifically targeting DNA gyrase, an enzyme crucial to bacterial DNA replication, it effectively demonstrates strong antibacterial action against an extensive variety of Gram-positive as well as Gram-negative bacteria. This inhibition disrupts the replication process, contributing to its efficacy as an antimicrobial agent [3]. NOR has found extensive application in both veterinary and human medicine, in addition to its use in aquaculture [4]. However, a significant portion of NOR residues cannot be fully metabolized in human or animal bodies, resulting in their eventual discharge into the surrounding environment. Such residues may pose potential hazard to both aquatic ecosystems and public health [4]. Due to the limitations of conventional wastewater treatment processes, a significant portion of antibiotics, such as NOR, can persist in treated wastewater effluents [5]. This poses a substantial risk of environmental contamination as these effluents are discharged into water bodies [5].

As a result, it is imperative to create efficient strategies for eliminating antibiotics from wastewater to mitigate the potential ecological and public health implications. Researchers have explored numerous wastewater

treatment techniques aimed at the efficient elimination of pollutants, including adsorption [1,6,7], adsorption-photo catalysis [8], membrane filtration [9], bioremediation [10,11], and Fenton reaction [12]. Among these methods, adsorption stands out as a highly cost-effective treatment approach, distinguished by its operational simplicity, cost-effectiveness, and broad applicability to various pollutants [5,13,14].

The ability of various metal-organic frameworks (MOFs) to adsorb antibiotics is the subject of ongoing research [15]. MOFs represent a distinct category of crystalline substances that result from the self-assembly process between clusters of metal ions and organic ligands. Their exceptional versatility, stemming from their ability to undergo chemical and structural modification, makes them highly promising for applications in adsorption and separation technologies [16]. The potential of MOFs for antibiotic elimination is attracting increasing attention [17,18]. One type of MOF is Zeolitic Imidazolate Frameworks (ZIFs), which are distinguished by a porous structure resembling zeolite. Due to its extraordinary heat and chemical resistance, cost-effectiveness, and simplicity of preparation, Zeolitic Imidazolate Framework-8 (ZIF-8) has become one of the most well-known ZIFs [1,15]. ZIF-8, created when zinc clusters are linked with the organic ligand 2-methylimidazole, exhibits a sodalite (SOD) framework composed of 1.2 nm cages with 3.4 Å pore sizes [4].

The synthesis conditions significantly influence the physicochemical characteristics of ZIF-8, such as its crystalline structure, particle size, pore structure, surface area, and morphology [19]. Several research efforts have focused on understanding how synthesis parameters, including the ligand-to-metal ratio, addition of auxiliary agents, temperature, and solvent type, contribute to the effective preparation of ZIF-8 [19]. For instance, Malekmohammadi *et al.* [19] found that the type of solvent, crystallization temperature, and ligand content, significantly impacted the textural properties and phase integrity of the prepared ZIF-8. Notably, ZIF-8 synthesized using methanol at 130 °C with a ligand-to-metal ratio of 2 exhibited a predominantly rhombic dodecahedron shape, while the aqueous synthesis at 25 °C with a ligand-to-metal ratio of 4 yielded a blend of rhombic dodecahedron and truncated cubic [19]. Santoso *et al.* [20] found that ZIF-8 nanoparticles prepared using two different solvents, N,N-Dimethylformamide (DMF) and acetic acid (AA), produced smaller

particle size of ZIF-8 (AA) (\sim 65 nm), than ZIF-8 (DMF) (\sim 2 µm) and enhanced mesoporosity, characterized by an elevated mesopore volume of 0.166 mLg⁻¹ and larger pore diameters (2.76 nm), while maintaining a moderate surface area (500 m²g⁻¹). In contrast, ZIF-8 (DMF) exhibited a microporous structure with an impressive surface area (1000 m²g⁻¹) and superior methylene blue adsorptive capacity, which was ascribed to the features of mesopores, highlighting the importance of pore structure in enhancing adsorption performance [20]. These profound insights from different studies emphasized the influence and importance of solvent types on ZIF-8 synthesis as well as their role in promoting adsorption.

Although previous studies have explored the effect of solvents on the physico-chemical properties of ZIF-8, there is still a lack of in-depth analysis on how solvent type systematically regulates the adsorption performance of ZIF-8 on NOR and its quantitative correlation with adsorption performance have not been fully revealed. This study aims to fill this gap by comparing the synthesis of ZIF-8 using water and methanol, providing a direct experimental basis for solvent selection. The prepared materials were characterized through various techniques, including FTIR, SEM-EDX, XRD, and BET, to assess their structural and physico-chemical properties. Additionally, the adsorption performance, including adsorption isotherms, kinetics, and thermodynamics, was thoroughly examined to determine the materials' effectiveness in removing pollutants and providing valuable insights for their potential use in environmental remediation applications. The study also explores the impact of different solvent-type on ZIF-8's adsorption capacity, offering guidance for selecting optimal solvents in future applications. Ultimately, the results aid in the creation of more effective materials for treating pharmaceutical contamination in wastewater.

EXPERIMENTAL METHODOLOGY

Chemicals

2-Methylimidazole (C₄H₆N₂, > 98%) and NOR (C₁₆H₁₈FN₃O₃, >98%) were supplied by Macklin Biochemicals (Shanghai, China). The suppliers were Tianjin Damao Chemical Reagents Ltd. for Zinc nitrate hexahydrate

 $(\text{Zn (NO}_3)_2. 6\text{H}_2\text{O}, > 99\%)$ and zinc sulfate heptahydrate $(\text{ZnSO}_4.7\text{H}_2\text{O}, > 99.5\%)$. Hydrochloric acid and sodium hydroxide of analytical grade were obtained from R&M Chemicals. All water-based solutions were made with deionized water.

Synthesis of Different ZIF-8

A refined method was followed in the synthesis of ZIF-8-W [21]. Briefly, solution A was prepared by dissolving 1.2078 g of ZnSO₄·7H₂O in 5 mL of deionized water. Additionally, solution B was prepared by dissolving 3.9411 g of 2-methylimidazole in 16 mL of deionized water. Subsequently, 1.6 mL of Solution A and 16 mL of Solution B were mixed, and deionized water was added to bring the total volume of the mixture to 50 mL. The mixture was stirred for 1 h at ambient temperature and centrifuged for 30 min at 5000 rpm to obtain ZIF-8 precipitate. Finally, the ZIF-8-W was obtained by washing the precipitate three times with deionized water, followed by drying in the oven for 12 h at 70 °C as depicted in Figure 1.

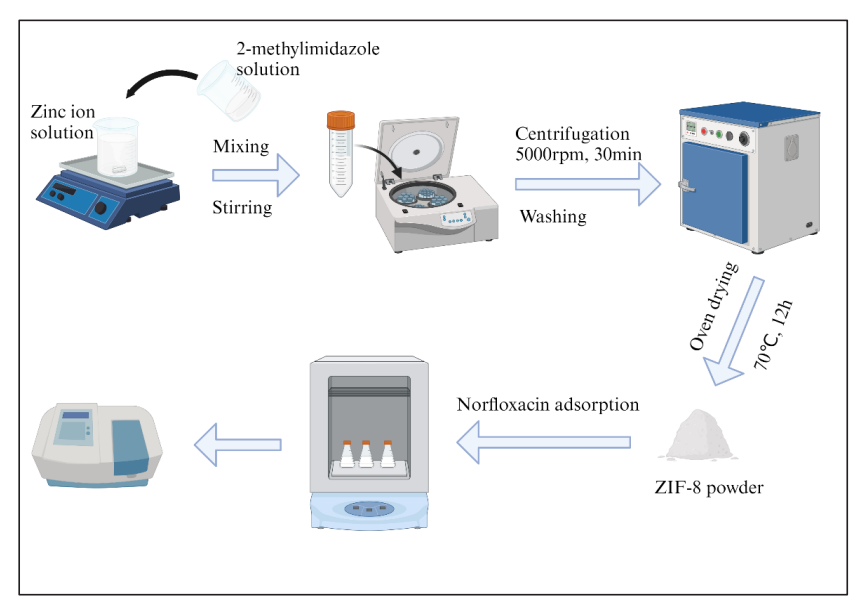


Figure 1: Schematic diagram of ZIF-8 synthesis and its adsorption experiment.

The synthesis method for ZIF-8-M followed the procedure previously reported [22]. In this process, zinc nitrate hexahydrate (0.366 g) and 2-methylimidazole (0.811 g) were dissolved separately in 25 mL of methanol. Hereafter these solutions were mixed and allowed for continuous stirring for 3 h at ambient temperature. Afterwards, the prepared material was cleaned using methanol 3 times and centrifuged for 30 min at 5000 rpm. After 12 h of drying at 70 °C, the final compound, ZIF-8-M, was obtained.

Characterization

With an X-ray Diffractometer (Rigaku Ultima IV XRD), the crystalline structure of the samples under investigation was described within the 2θ range of 5° to 80° at a scan rate of 8 min per degree. Monochromatic Cu K α radiation (1.5418A; 40kV) was used in the apparatus. Using Fourier Transform Infrared (FTIR) spectroscopy, which was performed in the 400-4000 cm $^{-1}$ spectral range, functional groups were analyzed. A Perkin Elmer UV-Vis/NIR Lamda 750 spectrophotometer was used to record the Ultraviolet-Visible (UV-Vis) absorption behavior, using BaSO4 as the reference material. A HITACHI SU3500 Scanning Electron Microscope (SEM) coupled with Energy Dispersive X-ray (EDX) running at an accelerating voltage of 15 kV was used to examine the samples' surface morphology and elemental composition. Brunauer-Emmett-Teller (BET) and Barrett-Joyner-Halenda (BJH) techniques were used to quantify the samples' surface area and pore size properties, separately, using N_2 adsorption-desorption isotherms carried out at 77 K.

Adsorption Experiments

The effectiveness of synthesized ZIF-8 in adsorbing NOR was conducted in batch mode. Initially, a 50 mL of NOR at 20 mg L⁻¹ and 50 mg of ZIF-8 were mixed and subjected to continuous agitation at 150 rpm in a thermoshaker. At specified time intervals (5, 10, 20, 30, 50, 70, 100, 130, and 160 min), samples were retrieved to quantify the remaining NOR concentration via UV-vis spectrophotometer at a wavelength of 278 nm. Each experiment was conducted in triplicate under identical conditions to guarantee high reproducibility. To better characterize the adsorption isotherms, additional batch experiments were conducted with a preliminary NOR concentration in the range of 10-70 mg L⁻¹ and all other experimental

parameters remain unchanged.

The amount of adsorbed NOR was quantified by employing Eq. (1) as follows:

$$q = (C_0 - C_t)v/m \tag{1}$$

The removal efficiency (expressed as a percentage, R%) was quantified by employing Eq. (2):

$$R(\%) = 100 \times (C_0 - C_t)/C_0 \tag{2}$$

where q is the ZIF-8 equilibrium adsorption capacity (mg g⁻¹), with C_0 and C_t representing the initial and final concentrations of NOR (mg L⁻¹) after a specified duration t. Additionally shown in the equation are the weight of ZIF-8 (g) and the volume of the NOR solution (L).

Adsorption Isotherms

In order to elucidate the mechanism of NOR elimination via ZIF-8, adsorption isotherm studies were conducted. In the batch experiments, a variety of preliminary NOR doses were tested, ranging from 10 to 70 mg L⁻¹ and fitted in the two most frequently used Langmuir and Freundlich isotherm adsorption models.

A chemical single-layer adsorption process is assumed to occur on the adsorbent's surface according to the Langmuir model [1]. This model is represented through Eq. (3):

$$\frac{C_e}{q_e} = \frac{C_e}{q_m} + \frac{1}{q_m K_L} \tag{3}$$

Here, q_e (mg g^{-1}) represents the equilibrium adsorption capacity of the adsorbent, indicating the amount of solute adsorbed per unit mass at equilibrium, C_e (mg L^{-1}) is the concentration of the solute remaining in the solution once equilibrium is reached, q_m (mg g^{-1}) represents the maximum adsorption capacity, which is the theoretical highest amount of solute the adsorbent can hold, K_L (mg L^{-1}) is the Langmuir adsorption constant, which reflects the affinity between the solute molecules and the adsorbent surface.

SCIENTIFIC RESEARCH JOURNAL

Conversely, the Freundlich model of isotherms is utilized to depict the reversible adsorption mechanism on heterogeneous interfaces [1]. The mathematical representation of this model is given by Eq. (4):

$$\ln q_e = \ln K_F + \frac{\ln C_e}{n} \tag{4}$$

Here, q_e (mg g^{-1}) signifies the equilibrium adsorption capacity of the adsorbent, C_e (mg L^{-1}) denotes the concentration of the solute remaining in the liquid phase at equilibrium, n is the empirical exponent that reflects the heterogeneity of the adsorption sites, K_F (mg^{1-1/n}L^{1/n}g⁻¹) represents the Freundlich adsorption equilibrium constant, where n is the empirical exponent that reflects the heterogeneity of the adsorption sites.

RESULTS AND DISCUSSION

XRD Analysis

In the XRD spectra of ZIF-8-W and ZIF-8-M prepared with various solvents depicted in Figure 2, eight distinct peaks were observed at diffraction angles of 7.3°, 10.4°, 12.7°, 14.7°, 16.4°, 18.0°, 24.5°, and 26.7°, aligning with the (011), (002), (112), (022), (013), (222), (233), and (134) crystallographic planes of ZIF-8.

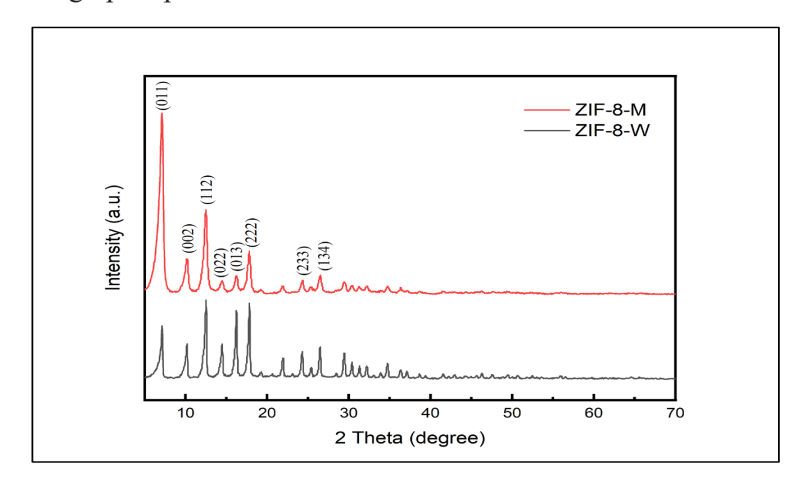


Figure 2: XRD spectra for ZIF-8-W and ZIF-8-M.

The samples acquired with two varied solvents align with the previously published data concerning ZIF-8 [21]. These results indicated successful synthesis of ZIF-8. The solvent exerted a significant influence on the crystallinity of the synthetic materials [19]. By employing ZIF-8-M as a benchmark, the relative crystallinity was determined according to Eq. (5) [19]. ZIF-8-M exhibited a higher relative crystallinity (1.00), whereas ZIF-8-W showed a lower relative crystallinity of 0.74, relative to ZIF-8-M

Relative crystallinity =
$$\frac{Peak \text{ intensity of the sample at (011, 112, 222) planes}}{Peak \text{ intensity of the references at (011, 112, 222) planes}}$$
 (5)

The results shown demonstrated that the ZIF-8-M sample synthesized in methanol exhibited high crystallinity, due to the low polarity and weak coordination ability of methanol. This result was aligned with the findings of others [19, 23]. Methanol, as a weakly coordinating solvent, slowed down the coordination rate of metal ions (Zn²⁺) with 2-methylimidazole ligands, thereby promoting the formation of an ordered lattice [24]. In contrast, the high polarity of water led to rapid nucleation and irregular growth, thus reducing crystallinity [23].

Using the Debye-Scherrer formula, the mean grain size (D) for ZIF-8-W and ZIF-8-M was determined, which is expressed as Eq. (6):

$$D = \frac{0.9\lambda}{\beta \cos\theta} \tag{6}$$

The formula comprises β , the full width at half-maximum (FWHM), λ , the incident X-ray's wavelength (1.54 Å), and θ , the diffraction angle for the peak with the highest intensity associated with the (011) plane. ZIF-8-M had an average grain size of 16.62 nm, while ZIF-8-W had an average of 46.74 nm.

SEM-EDX Analysis

The SEM analysis of the sample morphology revealed that ZIF-8-W exhibited a non-uniform particle structure, with grain sizes ranging approximately between 50.19 ± 6.40 nm, as depicted in Figure 3(a) [21]. In contrast, the ZIF-8-M sample prepared showed a uniform particle morphology, with particle sizes ranging roughly from 12.62 ± 1.11 nm, as illustrated in Figure 3(b) [22]. The uniform morphology of ZIF-8-M

SCIENTIFIC RESEARCH JOURNAL

was related to the lower interfacial tension of methanol. The lower surface tension of methanol allowed the crystals to spread evenly during growth and reduced particle aggregation [20]. The high dielectric constant of water triggered rapid precipitation, resulting in the non-uniform particle distribution of ZIF-8-W. Table 1 showed the elemental analysis of ZIF-8-W and ZIF-8-M. ZIF-8-M has higher a higher carbon and oxygen content in both weight and atomic percentage compared to ZIF-8-W. This suggests a greater organic framework formation in ZIF-8-M, which could be attributed to better crystallization of the imidazolate linkers in methanol [1].

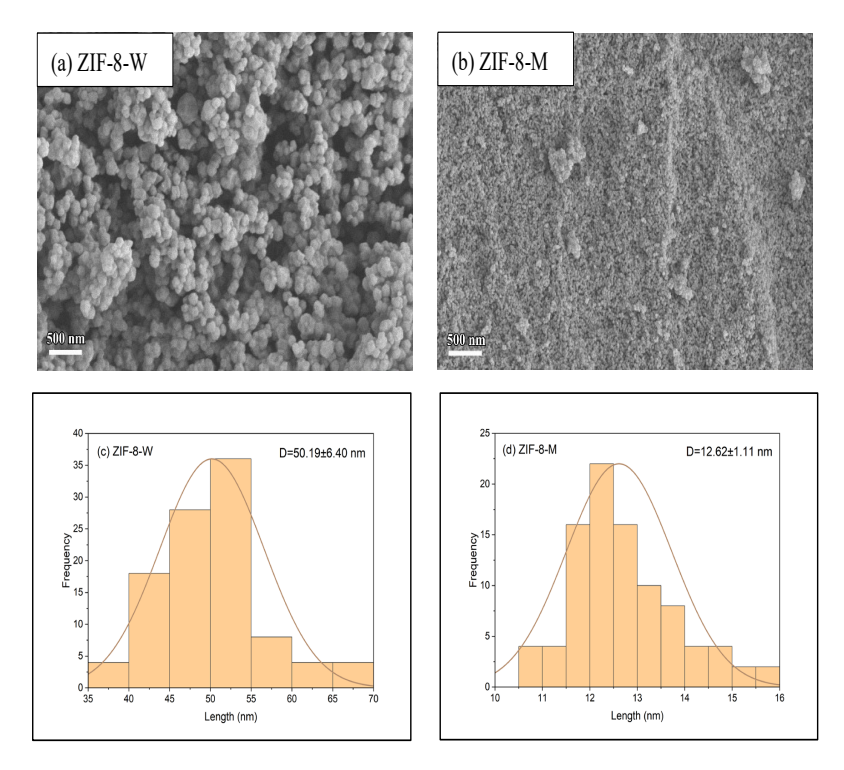


Figure 3: SEM images of (a) ZIF-8-W, (b) ZIF-8-M and particle distributions of (c) ZIF-8-W, (d) ZIF-8-M.

Sample/	ZIF-	8-W	ZIF-8-M				
Element	Weight, %	Atomic, %	Weight, %	Atomic, %			
С	49.23	64.84	57.36	69.33			
N	16.78	18.94	12.61	13.07			
0	10.71	10.59	15.94	14.47			
Zn	23.28	5.63	14.09	3.13			

Table 1: Elemental analysis results of ZIF-8-W and ZIF-8-M.

FTIR Analysis

The ZIF-8-W FTIR and ZIF-8-M FTIR spectra displayed in Figure 4 exhibited characteristic vibrational bands at 1425 cm⁻¹, 1428 cm⁻¹, 993 cm⁻¹, and 994 cm⁻¹, indicative of C-N stretching. Furthermore, imidazole bending was assigned to the bands at 1145 cm⁻¹, 1146 cm⁻¹, 1308 cm⁻¹, and 1309 cm⁻¹, whereas Zn-N stretching was associated with a significant band at 421 cm⁻¹. These findings were aligned with previous studies on ZIF-8 synthesis [21]. Remarkably, it was discovered that ZIF-8 samples made with various solvents had identical FTIR spectra [23].

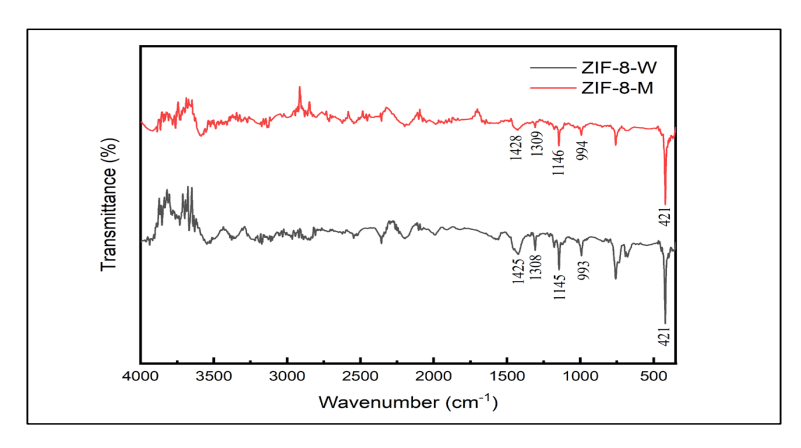


Figure 4: FTIR spectra of the synthesized ZIF-8-W and ZIF-8-M. BET Analysis

Nitrogen adsorption-desorption tests were conducted to get insight into ZIF-8's surface textural properties. As depicted in Figure 5(a), both ZIF-8-W and ZIF-8-M exhibited typical Type I hysteresis loops, indicative of their microporous structure. This finding is in agreement with previous

work [15]. Table 2 shows a comprehensive analysis of the structural parameters. The ZIF-8-W sample, synthesized using water, demonstrated a pore volume of 0.178 cm³g⁻¹ and a BET surface area of 318.609 m²g⁻¹. In contrast, ZIF-8-M exhibited a pore volume of 0.254 cm³g⁻¹ and a higher BET surface area of 557.832 m²g⁻¹. The pore structure and superior surface area of ZIF-8-M provided numerous adsorption sites for NOR, leading to enhanced adsorption performance [22]. The benefits of increasing ZIF-8's surface area for its use as an adsorbent were clear [25]. It was worth noting that when substituting water with methanol as the solvent, ZIF-8 exhibited an increased surface area. This discovery was consistent with Malekmohammadi's research findings [19].

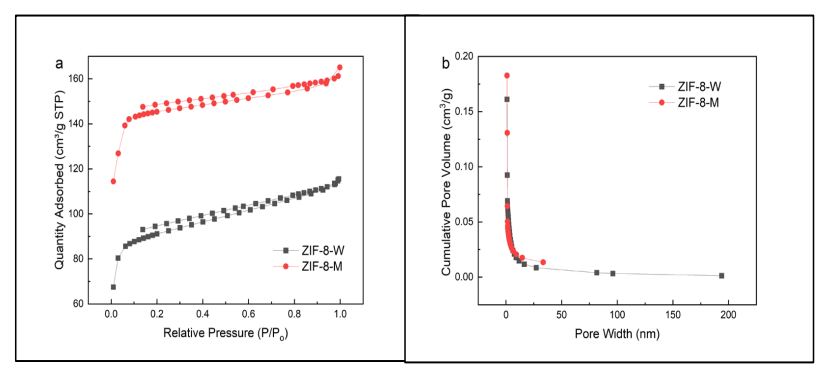


Figure 5: (a) N₂ adsorption-desorption isotherms; (b) Pore size distribution of the synthesized ZIF-8-W and ZIF-8-M.

	, , , , , , , , , , , , , , , , , , , 		
Sample	BET surface area (m² g-1)	Pore volume (cm³ g-1)	Average pore diameter (nm)
ZIF-8-W	318.609	0.178	2.231
ZIF-8-M	557.832	0.254	1.823

Table 2: Porosity properties of the synthesized ZIF-8-W and ZIF-8-M.

Adsorption Performance

As illustrated in Figure 6, adsorption performance progressively raised with the extension of the adsorption period until reaching equilibrium. ZIF-8-M exhibited superior removal efficiency (86.49%) and adsorption capacity (17.30 mgg⁻¹) compared to ZIF-8-W, which achieved respective values of 53.01% and 10.60 mgg⁻¹. This observation was likely due to the

increased surface area (557.832 m²g⁻¹) and pore structure (0.254 cm³g⁻¹) in ZIF-8-M. ZIF-8-M's high specific surface area and well-developed pore structure offered abundant adsorption sites for NOR, significantly improving its adsorption performance [22].

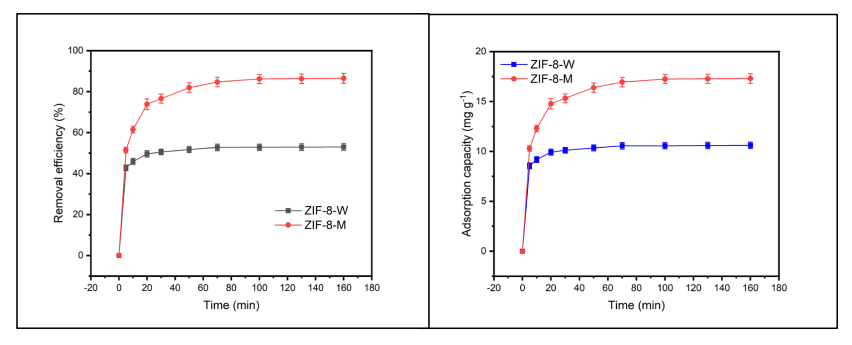


Figure 6: Adsorption performance of NOR on ZIF-8-W and ZIF-8-M (Conditions: dose 1 g L^{-1} , C_0 20 mg L^{-1} , T 298.15 K).

Adsorption Isotherms Analysis

The Freundlich model provided a more accurate description of the NOR adsorption isotherms on ZIF-8-W and ZIF-8-M (Figure 7 and Table 3). This is supported by the higher R² values (0.991 for both materials) compared to the Langmuir model ($R^2 = 0.950$ for ZIF-8-W and 0.960 for ZIF-8-M). The Langmuir model proved inadequate in representing the isotherm curves, whereas the Freundlich model demonstrated a strong correlation with the adsorption experimental data, as evidenced by the high linear correlation coefficient (R2). NOR was adsorbed onto ZIF-8-W and ZIF-8-M via a multi-layer adsorption process. The data obtained corresponds to the findings from the kinetic parameter fitting process, implying that the adsorption mechanism was chemical adsorption. This discovery was consistent with the adsorption isotherm findings conducted by other researchers for the removal of antibiotics through adsorption [1]. Both ZIF-8-W and ZIF-8-M had 1/n values ranging from 0 to 1, suggesting favorable adsorption processes [14]. Additionally, ZIF-8-M exhibited a higher KF value compared to ZIF-8-W, indicating a stronger adsorption affinity between ZIF-8-M and NOR compared to the interaction between ZIF-8-W and NOR [14].

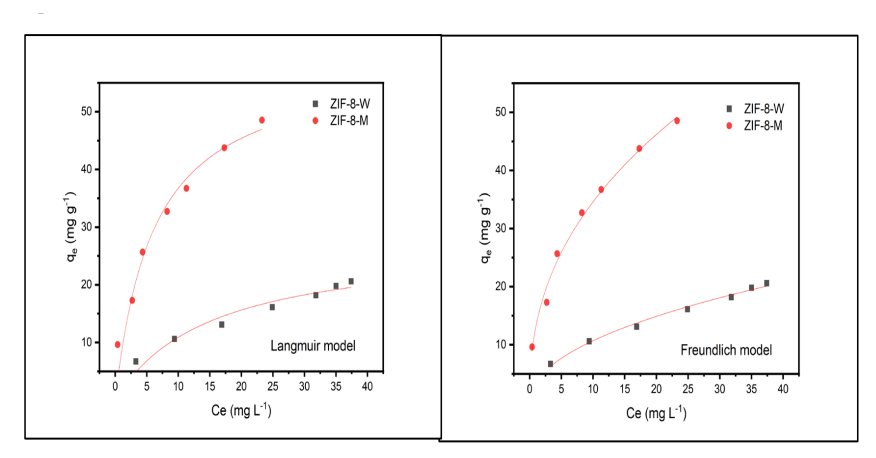


Figure 7: The adsorption isotherm curve for NOR modeled by Langmuir and Freundlich model (Conditions: dose 1 g L¹¹, C₀ 10-70 mg L¹¹, T 298.15 K).

Table 3: ZIF-8-W and ZIF-8-M isotherm parameters for NOR adsorption.

Adsorbents	Langmuir				Freundlich		
	K _L (L mg ⁻¹)	q _{max} (mgg ⁻¹)	R ²	Z	K_{F} (mg ^{1-1/n} L ^{1/n} g ⁻¹)	R ²	
ZIF-8-W	0.07	27.48	0.950	2.09	3.55	0.991	
ZIF-8-M	0.16	59.35	0.960	2.40	13.23	0.991	

Kinetics Analysis

The adsorption kinetics of NOR on ZIF-8-W and ZIF-8-M adsorbents were analyzed using the widely used pseudo-first-order kinetic model and pseudo-second-order kinetic model in order to explore the adsorption mechanism, as formulated in Eq. (7) and (8).

Pseudo-first-order model:

$$\ln(q_e - q_t) = \ln q_e - K_1 t \tag{7}$$

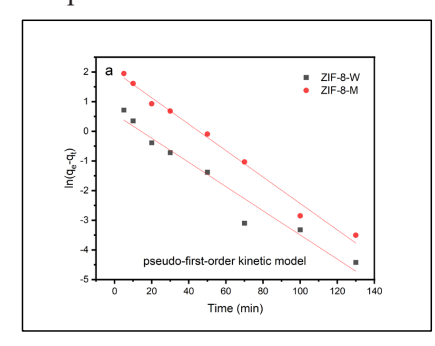
Pseudo-second-order model:

$$\frac{t}{q_t} = \frac{t}{q_e} + \frac{1}{K_2 q_e^2} \tag{8}$$

Here, q_c (mg g⁻¹) represents the equilibrium adsorption capacity of NOR;

 $q_{_{t}}(mgg^{-1})$ refers to the time-varying adsorption capacity, which shows the amount of NOR adsorbed at any given time during the process; $k_{1}(min^{-1})$ is the rate constant for the pseudo-first-order kinetic model, describing the rate of adsorption based on the concentration of the adsorbate; and k_{2} (gmg⁻¹ min⁻¹) is the rate constant for the pseudo-second-order model, which assumes that the adsorption rate depends on the adsorbate already on the adsorbent surface.

The experimental data were fitted into the pseudo-first-order and pseudo-second-order kinetic models as depicted in Figure 8(a, b). During the initial 30 min, a rapid adsorption rate on the ZIF-8 surface was observed because of the abundance of active adsorption sites. Nonetheless, the adsorption rate slowed down from 30 to 90 min, ultimately achieving equilibrium at 90 min. The adsorption of NOR onto ZIF-8-W and ZIF-8-M was well described by the pseudo-second-order model, and yielded a high correlation coefficient of 0.999, which showed a strong agreement with the experimental data. This implied that chemisorption was the main adsorption mechanism [2]. In Table 4, the pseudo-second-order kinetic rate constant of ZIF-8-M ($k_2 = 0.0136 \text{ g mg}^{-1}\text{min}^{-1}$) was significantly lower than that of ZIF-8-W (0.0615 g mg⁻¹ min⁻¹), indicating that the adsorption process of ZIF-8-M relied more on chemical bonding rather than physical diffusion, which was consistent with its high specific surface area and chemical adsorption mechanism. The kinetic analysis from earlier research on antibiotic adsorption is in agreement with our findings [1]. Consequently, it can be concluded that the pseudo-second-order model better explain the adsorption of NOR onto ZIF-8.



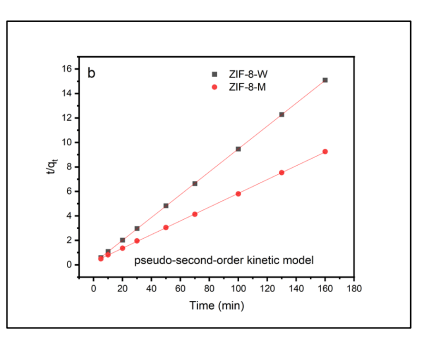


Figure 8: Linear fitting of experimental adsorption kinetics data using the pseudo-first-order and pseudo-second-order kinetic models (Conditions: dose 1 gL¹, C₀ 20 mgL¹, T 298.15 K).

Adsorbents	Pseudo-first-order model			Pseudo-second-order model			
	k ₁ (min ⁻¹)	q _{e1} (mg g ⁻¹)	R ²	k ₂ (g mg ⁻¹ min ⁻¹)	q _{e2} (cal) (mg g ⁻¹)	R ²	
ZIF-8-W	0.0408	1.78	0.959	0.0615	10.71	0.999	
ZIF-8-M	0.0446	7.47	0.989	0.0136	17.81	0.999	

Table 4: The adsorption kinetics of NOR onto ZIF-8-W and ZIF-8-M.

Thermodynamic Studies Analysis

The role of temperature in the adsorption of NOR onto ZIF-8-W and ZIF-8-M was investigated by analyzing thermodynamic parameters, including ΔGo , ΔSo , and ΔHo . These parameters were calculated using Eq. (9)-(11). The preliminary concentration of NOR used in the thermodynamic studies was 20 mgL⁻¹. Three different temperatures at 298 K, 308 K, and 318 K, respectively were used in the experiment. Subsequently, the data obtained were applied to determine the thermodynamic variables based on the equations mentioned:

$$\Delta G = -RT \ln K \tag{9}$$

$$K = \frac{q_e}{C_e} \tag{10}$$

$$\ln K = -\frac{\Delta H}{RT} + \frac{\Delta S}{R} \tag{11}$$

Here, ΔG represents the variation in Gibbs free energy (kJ mol⁻¹); ΔH signifies the total enthalpy change (kJ mol⁻¹), reflecting the heat absorbed or released during adsorption; ΔS represents the entropy change (kJ mol⁻¹ k⁻¹), indicating the disorder or randomness of the process; R is the universal gas constant (8.314 J mol⁻¹ K⁻¹), used in thermodynamic calculations; K denotes the thermodynamic equilibrium constant (L mol⁻¹); q_e (mg g⁻¹) refers to the equilibrium adsorption capacity; C_e (mg L⁻¹) denotes the equilibrium concentration in the aqueous phase, used to calculate adsorption.

In Table 5, the computational parameters indicated that ΔG remained negative throughout, indicating that the adsorption process occurs spontaneously. The free energy marginally decreased when the temperature

rose from 298 K to 318 K, suggesting that elevated temperatures favoured the enhancement of adsorption. The enthalpy changes (Δ H) for ZIF-8-W and ZIF-8-M were 3.98 and 17.20 kJ mol⁻¹, correspondingly. These positive values implied that the adsorption of NOR followed an endothermic process and was supported by the experimental results which demonstrated that the increased of adsorption as the temperature rose [1].

Table 5: Thermodynamic characteristics of ZIF-8-W as well as ZIF-8-M adsorption for NOR.

Adsorbents	ΔGo (kJ mol ⁻¹)			ΔHo (kJ mol ⁻¹)	ΔSo (kJ mol ⁻¹ k ⁻¹)
	298 K	308 K	318 K		
ZIF-8-W	-0.28	-0.41	-0.57	3.98	0.014
ZIF-8-M	-4.60	-5.02	-6.07	17.20	0.072

A summary table comparing the adsorption performance of ZIF-8 and its composites with previous literature (Table 6), is presented alongside the findings in this study. It is evident that the as-prepared ZIF-8 in the present work shows great potential as effective absorbent in removing NOR.

Table 6: Comparison of ZIF-8 and its composites' adsorption performance with previous literature.

Adsorbent	Pollutant	Adsorption capacity (mg g ⁻¹)	References
ZIF-8-W	NOR	21.10	This study
ZIF-8-M	NOR	46.74	This study
ZIF-8 Methylene blue		47.90	[24]
ZIF-8 Tetracycline		90.00	[15]
ZIF-8	Ofloxacin	194.10	[16]
ZIF-8	As(III)	72.00	[26]
Fe₃O₄/ZIF-8	As(III)	21.12	[27]
ZIF-8@CA	Cr(VI)	41.80	[28]

Notes: CA: Calcium Alginate

CONCLUSION

This study successfully examined the influence of different solvents during the synthesis of ZIF-8 affecting its physicochemical properties and adsorption effectiveness towards NOR. Compared to ZIF-8-W, ZIF-8-M exhibited superior characteristics with higher crystallinity, larger pore volume, and greater BET surface area. These improved properties contributed to a significantly higher adsorption capacity and removal efficiency for NOR, with an adsorption capacity of 17.30 mgg⁻¹ and NOR removal efficiency of 86.49%, respectively. Isotherm and kinetic analyses suggested that NOR adsorption follows a Freundlich model and pseudo-second-order kinetics, suggesting multilayer adsorption and chemisorption mechanisms. These findings point to multilayer adsorption as the predominant mechanism governing the removal of NOR. The adsorption reaction's spontaneous and endothermic characteristics are supported by experimental thermodynamic analysis. The adsorption isotherms, kinetics, and thermodynamics of ZIF-8 synthesized using distinct solvents exhibited minimal variation underline the critical role of synthesis solvents in optimizing ZIF-8's structural and functional properties, which directly affect its adsorption performance. The study demonstrates the potential of ZIF-8, particularly the methanolsynthesized form, as an efficient substance for eliminating antibiotic pollutants, such as NOR, from wastewater. This work can be expanded to other polar or non-polar solvents to examine the effects of complex coexisting pollutants in actual wastewater on adsorption efficiency, as well as the regeneration performance and long-term stability of ZIF-8. Solving these challenges is crucial for the practical application of ZIF-8 adsorbent materials in real wastewater treatment, making it a promising candidate for solving emerging environmental challenges related to pharmaceutical pollutants.

ACKNOWLEDGEMENTS

The authors would like to express their gratitude to the College of Engineering, Universiti Teknologi MARA, for their support in completing this research.

REFERENCES

- [1] L. Zhou, N. Li, G. Owens & Z. Chen, 2019. Simultaneous removal of mixed contaminants, copper and norfloxacin, from aqueous solution by ZIF-8, *Chemical Engineering Journal*, 362, 628 637.
- [2] S. Saghir & Z. Xiao, 2021. Facile preparation of metal-organic frameworks-8 (ZIF-8) and its simultaneous adsorption of tetracycline (TC) and minocycline (MC) from aqueous solutions, *Materials Research Bulletin*, 141, 111372.
- [3] W. Liu, J. Zhang, C. Zhang & L. Ren, 2011. Sorption of norfloxacin by lotus stalk-based activated carbon and iron-doped activated alumina: Mechanisms, isotherms and kinetics, *Chemical Engineering Journal*, 171, 431 438.
- [4] M. A. Nazir, S. Ullah, M. U. Shahid, I. Hossain, T. Najam, M. A. Ismail, A. U. Rehman, M. R. Karim & S. S. A. Shah, 2025. Zeolitic imidazolate frameworks (ZIF-8 & ZIF-67): Synthesis and application for wastewater treatment, *Separation and Purification Technology*, 356, 129828.
- [5] T. Chahm, L. F. De Souza, N. R. Dos Santos, B. A. Da Silva & C. A. Rodrigues, 2019. Use of chemically activated termite feces a low-cost adsorbent for the adsorption of norfloxacin from aqueous solution, *Water Science and Technology*, 79, 291 301.
- [6] V. T. Nguyen, T. D. H. Vo, T. B. Nguyen, N. D. Dat, B. T. Huu, X. C. Nguyen, T. Tran, T. N. C. Le, T. G. H. Duong, M.H. Bui, C. D. Dong & X. H Bui, 2022. Adsorption of norfloxacin from aqueous solution on biochar derived from spent coffee ground: Master variables and response surface method optimized adsorption process, *Chemosphere*, 288, 132577.
- [7] Y. Yang, Z. Zhong, J. Li, H. Du & Z. Li, 2022. Efficient with low-cost removal and adsorption mechanisms of norfloxacin, ciprofloxacin and ofloxacin on modified thermal kaolin: experimental and theoretical

- studies, Journal of Hazardous Materials, 430, 128500.
- [8] W. Liu, T. He, Y. Wang, G. Ning, Z. Xu, X. Chen, X. Hu, Y. Wu & Y. Zhao, 2020. Synergistic adsorption-photocatalytic degradation effect and norfloxacin mechanism of ZnO/ZnS@BC under UV-light irradiation, *Scientific Reports*, 10, 1 12.
- [9] M. Chen, S. G. J. Heijman & L. C. Rietveld, 2024. Ceramic membrane filtration for oily wastewater treatment: Basics, membrane fouling and fouling control, *Desalination*, 583, 117727.
- [10] S. Elhamji, K. Sbihi, S. Lghoul, K. Aziz, A. E. Maallem, T. A. Kurniawan & F. Aziz, 2025. Addressing the challenge of heavy metal contamination in aquatic environment: Harnessing the bioremediation potential of Navicula permitis diatom for wastewater treatment, *Biomass and Bioenergy*, 197, 107776.
- [11] E. Beltrán-Flores, P. Blánquez, A. M. Gorito, M. Sarrà & A. M. T. Silva, 2024. Combining fungal bioremediation and ozonation for rinse wastewater treatment, *Science of the Total Environment*, 912, 169198.
- [12] Y. Jiang, J. Ran, K. Mao, X. Yang, L. Zhong, C. Yang, X. Feng & H. Zhang, 2022. Recent progress in Fenton/Fenton-like reactions for the removal of antibiotics in aqueous environments, *Ecotoxicology and Environmental Safety*, 236, 113464.
- [13] Y. Wang, W. Yu, Z. Chang, C. Gao, Y. Yang, B. Zhang, Y. Wang & B. Xing, 2022. Effects of dissolved organic matter on the adsorption of norfloxacin on a sandy soil (fraction) from the Yellow River of Northern China, *Science of the Total Environment*, 848, 157495.
- [14] Y. Zhang, F. Ni, J. He, F. Shen, S. Deng, D. Tian, Y. Zhang, Y. Liu, C. Chen & J. Zou, 2021. Mechanistic insight into different adsorption of norfloxacin on microplastics in simulated natural water and real surface water, *Environmental Pollution*, 284, 117537.

- [15] K. Li, M. Chen, L. Chen, S. Zhao, W. Pan, P. Li & Y. Han, 2024. Adsorption of tetracycline from aqueous solution by ZIF-8: Isotherms, kinetics and thermodynamics, *Environmental Research*, 241, 117588.
- [16] R. Yu & Z. Wu, 2020. High adsorption for ofloxacin and reusability by the use of ZIF-8 for wastewater treatment, *Microporous and Mesoporous Materials*, 308, 110494.
- [17] K. Shi, H. Su, K. Liu, Y. Zhang & J. Zhu, 2025. Green room-temperature fabrication of phosphotungstic acid functionalized MOF-808 for efficient removal of cationic antibiotics, *Separation and Purification Technology*, 357, 130155.
- [18] N. Priyadarshini, K. Kumar Das, S. Mansingh & K. Parida, 2022. Facile fabrication of functionalised Zr co-ordinated MOF: Antibiotic adsorption and insightful physiochemical characterization, *Results in Chemistry*¹, 4, 100450.
- [19] M. Malekmohammadi, S. Fatemi, M. Razavian & A. Nouralishahi, 2019. A comparative study on ZIF-8 synthesis in aqueous and methanolic solutions: Effect of temperature and ligand content, *Solid State Sciences*, 91, 108 112.
- [20] E. Santoso, R. Ediati, Z. Istiqomah, D. O. Sulistiono, R. E. Nugraha, Y. Kusumawati, H. Bahruji & D. Prasetyoko, 2021. Facile synthesis of ZIF-8 nanoparticles using polar acetic acid solvent for enhanced adsorption of methylene blue, *Microporous and Mesoporous Materials*, 310, 110620.
- [21] S. Angela, V. B. Lunardi, K. Kusuma, F. E. Soetaredjo, J. N. Putro, S. P. Santoso, A. E. Angkawijaya, J. Lie, C. Gunarto, A. Kurniawan & S. Ismadji, 2021. Facile synthesis of hierarchical porous ZIF-8@TiO₂ for simultaneous adsorption and photocatalytic decomposition of crystal violet, Environmental Nanotechnology, *Monitoring & Management*, 16, 100598.

- [22] W. Yang, Y. Kong, H. Yin & M. Cao, 2023. Study on the adsorption performance of ZIF-8 on heavy metal ions in water and the recycling of waste ZIF-8 in cement, *Journal of Solid State Chemistry*, 326, 124217.
- [23] E. L. Bustamante, J. L. Fernández & J. M. Zamaro, 2014. Influence of the solvent in the synthesis of zeolitic imidazolate framework-8 (ZIF-8) nanocrystals at room temperature, *Journal of Colloid and Interface Science*, 424, 37 43.
- [24] G. Zhang, Y. Wang, X. Wang, B. Jiang, Y. Liu & H. Song, 2023. Rapid and facile synthesis of micro-mesoporous ZIF-8 materials with enhanced adsorption of methylene blue, *Polyhedron*, 244, 116620.
- [25] A. A. Jameh, T. Mohammadi, O. Bakhtiari & M. Mahdyarfar, 2019. Synthesis and modification of Zeolitic Imidazolate Framework (ZIF-8) nanoparticles as highly efficient adsorbent for H2S and CO2 removal from natural gas, Journal of Environmental Chemical Engineering, 7, 103058.
- [26] M. Massoudinejad, A. Mohammadi, S. Sadeghi, M. Ghaderpoori, S. Sahebi & A. Alinejad, 2022. Arsenic adsorption over dodecahedra ZIF-8 from solution aqueous: modelling, isotherms, kinetics and thermodynamics. *International Journal of Environmental Analytical* Chemistry, 102, 855 871.
- [27] Q. Wu, D. Wang, C. Chen, C. Peng, D. Cai & Z. Wu, 2021. Fabrication of Fe₃O₄/ZIF-8 nanocomposite for simultaneous removal of copper and arsenic from water/soil/swine urine, *Journal of Environmental Management*, 290, 112626.
- [28] S. Bo, W. Ren, C. Lei, Y. Xie, Y. Cai, S. Wang, J. Gao, Q. Ni & J. Yao, 2018. Flexible and porous cellulose aerogels/zeolitic imidazolate framework (ZIF-8) hybrids for adsorption removal of Cr(IV) from water, *Journal of Solid State Chemistry*, 262, 135 141.